Free Radical Biology & Medicine 52 (2012) 962–969

Contents lists available at SciVerse ScienceDirect

Free Radical Biology & Medicine

journal homepage: www.elsevier.com/locate/freeradbiomed

Original Contribution

Trimer hydroxylated quinone derived from apocynin targets cysteine residues of p47^{phox} preventing the activation of human vascular NADPH oxidase

Mauricio Mora-Pale [a], Seok Joon Kwon [a], Robert J. Linhardt [b,c], Jonathan S. Dordick [a,c,d,*]

[a] Department of Chemical and Biological Engineering, Rensselaer Polytechnic Institute, Center for Biotechnology and Interdisciplinary Studies, Troy, NY 12180, USA
[b] Department of Chemistry and Chemical Biology, Rensselaer Polytechnic Institute, Center for Biotechnology and Interdisciplinary Studies, Troy, NY 12180, USA
[c] Department of Biology, Rensselaer Polytechnic Institute, Center for Biotechnology and Interdisciplinary Studies, Troy, NY 12180, USA
[d] Department of Biomedical Engineering, Rensselaer Polytechnic Institute, Center for Biotechnology and Interdisciplinary Studies, Troy, NY 12180, USA

ARTICLE INFO

Article history:
Received 5 September 2011
Revised 14 December 2011
Accepted 16 December 2011
Available online 29 December 2011

Keywords:
Human vascular NADPH oxidase
Enzyme inhibition
Apocynin-derived oligophenols
p47^{phox}
p22^{phox}
Free radicals

ABSTRACT

Enzymatically derived oligophenols from apocynin can be effective inhibitors of human vascular NADPH oxidase (Nox). An isolated trimer hydroxylated quinone (IIIHyQ) has been shown to inhibit endothelial NADPH oxidase with an IC_{50} ~30 nM. In vitro studies demonstrated that IIIHyQ is capable of disrupting the interaction between p47^{phox} and p22^{phox}, thereby blocking the activation of the Nox2 isoform. Herein, we report the role of key cysteine residues in p47^{phox} as targets for the IIIHyQ. Incubation of p47^{phox} with IIIHyQ results in a decrease of ~80% of the protein free cysteine residues; similar results were observed using 1,2- and 1,4-naphthoquinones, whereas apocynin was unreactive. Mutants of p47^{phox}, in which each Cys was individually replaced by Ala (at residues 111, 196, and 378) or Gly (at residue 98), were generated to evaluate their individual importance in IIIHyQ-mediated inhibition of p47^{phox} interaction with p22^{phox}. Specific Michael addition on Cys196, within the N–SH3 domain, by the IIIHyQ is critical for disrupting the p47^{phox}–p22^{phox} interaction. When a C196A mutation was tested, the IIIHyQ was unable to disrupt the p47^{phox}–p22^{phox} interaction. However, the IIIHyQ was effective at disrupting this interaction with the other mutants, displaying IC_{50} values (4.9, 21.0, and 2.3 μM for the C111A, C378A, and C98G mutants, respectively) comparable to that of wild-type p47^{phox}.

Reactive oxygen species (ROS) regulate cellular signaling, affecting several aspects of cellular function, such as proliferation, migration, gene expression, and cell death. Several enzymes are expressed in the vasculature and contribute to ROS generation (e.g., endothelial nitric oxide synthases, cytochrome P450s, xanthine oxidase, and NADPH oxidases). Among this group of enzymes, NADPH oxidases catalyze superoxide ($O_2^{\bullet-}$) synthesis that triggers formation of ROS (e.g., hydrogen peroxide and hydroxyl radical), species that play a critical role in the development of oxidative stress-related cardiovascular diseases, including ischemia, restenosis, stroke, and arteriosclerosis [1–4]. At least three isoforms of NADPH oxidase (Nox) are expressed in vascular endothelial cells (ECs), Nox1, Nox2, and Nox4 [5,6], with Nox2 playing a critical role in ROS generation [7]. For example, Nox2 is upregulated approximately eightfold and its production of $O_2^{\bullet-}$ increases two- to threefold under induced oxidative stress [7]. Nox2 has 100% homology with the NADPH oxidase found in neutrophils, an enzyme involved in pathogen neutralization. Similar to the neutrophil enzyme, Nox2 undergoes a complex assembly of membrane- and cytosol-associated subunits to generate the activated enzyme. As depicted in Fig. 1A, translocation of cytosolic subunits (p47^{phox}, p67^{phox}, p40^{phox}, and Rac) occurs through binding to the membrane p22^{phox} and gp91^{phox} subunits [8–11]. Phosphorylation of serine residues in p47^{phox} results in conversion of inactive p47^{phox} into an active form of p47^{phox} and allows interaction of the p47^{phox} Src homology 3 (SH3) domain with proline-rich regions (PRRs) of p22^{phox} (Fig. 1B); this interaction is essential for activation of the Nox2 isoform [12,13].

Selective inhibitors of NADPH oxidase have been developed, some of which block the interaction of cytosolic subunits with membrane proteins, e.g., the flavonoid derivative S17834 (6,8-diallyl-5,7-dihydroxy-2-(2-allyl-3-hydroxy-4-methoxyphenyl)-1-*H*-benzo-[*b*]-pyran-4-one) and peptides such as the antibiotic PR-39 [14–16]; in vivo studies have shown that S17834 reduced aortic superoxide anion levels by 40% and aortic atherosclerotic lesions by 60% in apolipoprotein E-deficient mice [15]. In particular, polyphenols have gained significant attention because of their ability to bind proline-rich proteins [17,18]. Apocynin is a well-studied inhibitor of NADPH oxidase. Despite the growing number of studies with this phenolic compound, there remain questions about its precise role in NADPH oxidase inhibition. Some studies have revealed that apocynin is not a direct inhibitor of NADPH oxidase [19,20], whereas other studies suggest that apocynin acts as a simple antioxidant [19,21]. However, metabolism in vivo is expected to convert apocynin into reactive molecules, including oligophenols and their quinone analogs [22]. This has been observed in vivo. Thallas-Bonke and co-workers found that apocynin attenuates cytosolic superoxide generation in induced diabetic rats [23]. However, it is possible that the

* Corresponding author. Fax: +1 518 276 2207.
E-mail address: dordick@rpi.edu (J.S. Dordick).

0891-5849/$ – see front matter © 2011 Elsevier Inc. All rights reserved.
doi:10.1016/j.freeradbiomed.2011.12.015

observed effect on diabetic rats was due the conversion of apocynin into active metabolites. Indeed, Johnson et al. [20] and Kanegae et al. [24] found a dimer derived from apocynin to be an effective inhibitor, but its precise mode of action has not been determined, although oxidized oligophenolic compounds have been shown to bind to thiol groups and contribute to NADPH oxidase inhibition [25].

In our previous work, we reported on a broad complex mixture of derived oligophenols (up to heptamers) obtained from the peroxidase-catalyzed oxidation of apocynin and consisting of demethylated, hydroxylated, and quinone forms [26]. We isolated and fully characterized a trimer hydroxylated quinone (IIIHyQ), which showed strong inhibitory activity (IC_{50} 30 nM) against endothelial cell-based NADPH oxidase. The IIIHyQ was able to disrupt the in vitro interaction between a His-tagged $p47^{phox}$ (His-$p47^{phox}$) and a PRR peptide biotin-$p22^{phox}$ (IC_{50} 1.60 μM) [26]. A linear correlation existed between the inhibitory activity against EC NADPH oxidase and the ability to disrupt the interaction between biotin-$p22^{phox}$ and His-$p47^{phox}$, suggesting that apocynin-derived oligophenols are capable of preventing $p47^{phox}$–$p22^{phox}$ interaction in vivo. We now hypothesize that IIIHyQ may bind to critical cysteine residues of $p47^{phox}$, and in particular Cys196 located in the N–SH3 domain (Fig. 1C), via Michael adducts. Indeed, similar adducts are well known to occur between benzoquinone, naphthoquinone, anthraquinone, or dopamine quinone with Cys residues in proteins [27,28].

In this work, we have focused on gaining a more complete understanding of the mechanism of NADPH oxidase inhibition by apocynin-derived IIIHyQ. We evaluated the effect of IIIHyQ on the interaction of biotin-$p22^{phox}$ and His-$p47^{phox}$. Four $p47^{phox}$ mutants were expressed and purified, each containing a simple Cys replacement, thus sequentially eliminating potential targets for quinone binding. This approach resulted in the identification of Cys196 as a critical target for IIIHyQ leading to the potential prevention of $p47^{phox}$–$p22^{phox}$ interaction. We also evaluated the toxicity of the IIIHyQ compared with apocynin using PC-12 cells. This set of results establishes apocynin-derived oligophenols, and particularly metabolism-generated quinones, as candidates for potential therapeutic applications.

Materials and methods

Materials

Apocynin, soybean peroxidase (SBP), solvents, phosphate-buffered saline (PBS) tablets, H_2O_2, thiazolyl blue tetrazolium bromide, Tween 20, 3,3′,5,5′-tetramethylbenzidine (TMB), sodium caseinate, fetal bovine serum, heparin, and endothelial growth supplement were purchased from Sigma–Aldrich (St. Louis, MO, USA). Endothelial cells, PC-12 cells, and F12K medium were purchased from the ATCC (Manassas, VA, USA). *Escherichia coli* BL21(DE3), *E. coli* Top 10 competent cells, isopropyl-β-D-1-thiogalactopyranoside (IPTG), lucifer yellow iodoacetamide, and Ni-affinity column (Probond system) were purchased from Invitrogen (Carlsbad, CA, USA). Primers were obtained from Integrated DNA Technologies (Coralville, IA, USA). Antibodies were purchased from Upstate Biotechnology (Waltham, MA, USA). High-affinity streptavidin-coated 96-well plates were purchased from Pierce. LC–MS analyses were performed on a Shimadzu LCMS-2010A. Samples for LC–MS were separated in an Agilent Zorbax 300SB-C_{18} column (5 μm, 2.1×150 mm). Silica gel 230–400 mesh was purchased from Natland International Corp. (Morrisville, NC, USA). Thin-layer chromatography (TLC) plates were purchased from Merck (Whitehouse Station, NJ, USA). Microplate reader analyses were performed in a PerkinElmer HTS 7000 bioassay reader.

Enzymatic production of IIIHyQ from apocynin

IIIHyQ was synthesized via SBP-catalyzed oxidation of apocynin as described previously [26,29]. Briefly, apocynin (6 mmol) was dissolved in 5 ml of dimethylformamide and transferred to 490 ml phosphate buffer (50 mM, pH 7). SBP (5 ml of a 1 mg/ml solution) was added and the reaction was initiated by using a syringe pump to introduce H_2O_2 (30% w/v) at 0.1 ml/min for 12 min to afford 12 mmol H_2O_2. Finally, the reaction was stopped after 2 h. Soluble and precipitated phases were separated by centrifugation, and ethyl acetate was added to the supernatant to extract organic compounds. The extracted supernatant fraction was dried and stored at −20 °C under argon. Dried powder (290 mg) was dissolved in chloroform and loaded onto a silica gel column (15 g) and eluted with a gradient of petroleum ether:ethyl acetate (2:1 to 0:1). Unreacted apocynin was recovered in the early fractions (210 mg, R_f 0.62 with petroleum ether:ethyl acetate, 1:1) and further elution with pure ethyl acetate furnished the IIIHyQ as a white powder (14 mg, R_f 0.34 with petroleum ether:ethyl acetate, 1:1). TLC, NMR, and high-resolution mass spectrometry analyses were performed as previously reported [26].

Site-directed mutagenesis

Four mutants of His-$p47^{phox}$ were obtained by site-directed mutagenesis using the original plasmid (pET-28a (+), 5369 bp) used for production of recombinant His-$p47^{phox}$ wild type, C98G, C111A, C196A, and C378A. Primer design was performed following the guidelines of the QuickChange Lightning site-directed mutagenesis kit from Stratagene (Santa Clara, CA, USA); primers (reverse, R, and forward, F) for each mutant were C98GF, GGCACACTTACCGAGTAC*GGC*TCCACGCTCATGAGCCTGC, C98GR, GCAGGCTCATGAGCGTGGAGCCGTACTCGGTAAGTGTGCC; C111AF, CACCAAGATCTCCCGA*GCT*CCCCACCTCCTCGACTT, C111AR, AAGTCGAGGAGGTGGGGAGCTCGGGAGATCTTGGTG; C196AF, GAGCGGTTGGTGGTTC*GCT*CAGATGAAAGCAAAGC, C196AR, GCTTTGCTTTCATCTGAGCGAACCACCAACCGCTC; and C378AF, CCTCATCCTGAACCGC*GCT*AGCGAGAGCACCAAGC, C378AR, GCTTGGTGCTCTCGCTAGCGCGGTTCAGGATGAGG. The calculated melting temperature for each primer was ≥78 °C and the cycling parameters used for PCR are described in the instruction manual for the mutagenesis kit from Stratagene. After PCR, DNA was inserted into *E. coli* Top 10 cells and plasmid purified samples were sent for sequencing (MCLab, San Francisco, CA, USA) to confirm the correct mutations (see the supplementary material for primer design).

Production and purification of His-$p47^{phox}$ and biotin-p22

A proline-rich $p22^{phox}$ peptide N′-151PPSNPPPRPPAEARK165-C′, which was biotinylated at the N-terminus and amidated at the C-terminus, was obtained from Genemed Synthesis, Inc. (South San Francisco, CA, USA). A biotin group was attached through a 4-residue spacer consisting of SGSG. The purity of the peptide was 99.99%. EC-derived $p47^{phox}$ (wild type) DNA (6-His tagged) was obtained from the University of Albany and Stratton VA Medical Center and confirmed by DNA sequence analysis (University of Maine). His-$p47^{phox}$ proteins (wild type and mutants) were expressed in BL21(DE3) cells for 9 h using 0.5 mM IPTG at 35 °C. The protein was purified using a Ni-affinity column (ProBond System) and the purity (80%) was calculated with ImageJ software (U.S. National Institutes of Health).

Biotin-p22 and His-$p47^{phox}$ interaction

Interaction of His-$p47^{phox}$ (mutants and wild type) with the biotin-$p22^{phox}$ peptide was assessed using ELISA, as previously described [26,30]. Briefly, experiments were performed in high-affinity streptavidin-coated 96-well plates. To block nonspecific binding sites, each well was reblocked with 300 μl of PBS supplemented with 0.1% (v/v) Tween 20 and 1% sodium caseinate. To each well, 100 μl of biotin-$p22^{phox}$ (2 μM) peptide solution was added and incubated at room temperature for 1 h. After each well was washed four times

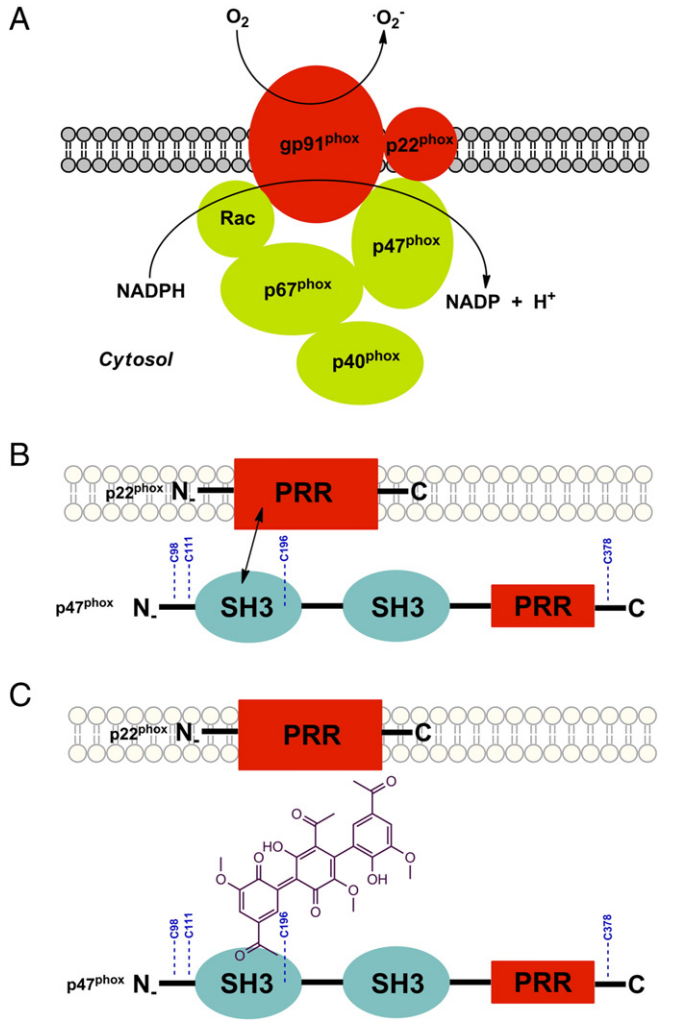

Fig. 1. (A) Active conformation of human vascular NADPH oxidase (Nox2 isoform); interaction between NADPH oxidase subunits $p22^{phox}$ and $p47^{phox}$. (B) N–SH3 domain of $p47^{phox}$ interacts with the proline-rich region (PRR) of $p22^{phox}$. (C) Cysteine at the 196 position of $p47^{phox}$ is the only cysteine located within the N–SH3 domain and is considered a critical target for quinones to prevent the interaction with $p22^{phox}$.

with 300 µl PBS–Tween 20 solution, 100 µl of 0.30 µM His-$p47^{phox}$ (in PBS–Tween solution containing 1% sodium caseinate) and IIIHyQ (0–1000 µM) were added to each well and incubated at room temperature for 1 h. Unbound IIIHyQ was removed by washing four times with 300 µl/well PBS–Tween 20 solution. The amounts of bound His-$p47^{phox}$ were quantified by adding 100 µl/well polyclonal goat anti-$p47^{phox}$ (diluted 1:2000 in PBS–Tween 20 solution containing 1% sodium caseinate) and incubating at room temperature for 1 h. Each well was washed four times with 300 µl PBS–Tween 20 solution and incubated with 100 µl/well horseradish peroxidase-conjugated rabbit anti-goat IgG secondary antibody (diluted 1:10,000 in PBS–Tween solution containing 1% sodium caseinate) at room temperature for 1 h. The plate was finally washed four times with 300 µl/well PBS–Tween solution and two additional washes with 300 µl/well PBS. Detection of peroxidase activity was performed with a ready-to-use TMB liquid substrate by adding 200 µl/well and incubating at room temperature for 30 min. The reaction was stopped with 100 µl/well 0.5 M H_2SO_4 solution and the absorbance was read at 450 nm in the microplate reader. All experiments were performed in triplicate and results were quantified from a standard curve of the interaction between biotin-$p22^{phox}$ (2 µM) and His-$p47^{phox}$ (0 to 0.5 µM). As positive controls, similar experiments were carried out using 1,2-naphthoquinone and 1,4-naphthoquinone, and phenylarsine oxide (PAO) was used as a negative control.

Quantification of cysteines

Reactivity of cysteines with quinones was determined using the fluorescent dye lucifer yellow iodoacetamide (following the protocol from Invitrogen). After purification in a Ni column, wild-type His-$p47^{phox}$ buffer was exchanged with 10 mM phosphate buffer (pH 7.0) using an Amicon ultracentrifuge filtration device (5 kDa MWCO). Wild-type His-$p47^{phox}$ (50 µM) was then incubated with the IIIHyQ, using 1,2- and 1,4-naphthoquinone as positive controls and apocynin as negative control (each compound at a final concentration of 500 µM). Lucifer yellow iodoacetamide (10 mM) was added and the reaction allowed to proceed at 4 °C overnight in the dark. To separate excess dye and protein conjugate, desalting spin columns (Zeba desalting spin columns, 7 kDa MWCO, 0.5 ml) were used three times until complete elimination of background fluorescence was achieved. After removal of the dye, protein concentration was determined by bicinchoninic acid protein assay. Finally, fluorescence spectra were taken at an excitation wavelength of 426 nm, showing a maximum of emission intensity ~530 nm.

Intracellular production of superoxide via dihydroethidium (DHE) staining

Qualitative determination of intracellular superoxide was performed via DHE fluorescence. DHE permeates endothelial cells and, in the presence of superoxide and other ROS, is oxidized to the red fluorescent 2-hydroxyethidium and ethidium, respectively, which are trapped with DNA resulting in bright red fluorescence. Although DHE can react with other ROS [31–33], the following method describes the generation of $O_2^{\bullet-}$ after the selective activation of vascular NADPH oxidase, which is the progenitor of other ROS (e.g., hydrogen peroxide and hydroxyl radical). Endothelial cells were incubated overnight in black, clear-bottom 96-well cell-binding surface plates in DMEM in the absence of phenol red. DMEM was removed and the cells were washed twice with PBS and then fresh DMEM (90 µl) was added. ECs were incubated for 30 min at 37 °C with phorbol myristate acetate (PMA; 1 µM) to activate NADPH oxidase. After consecutive washes with PBS and addition of fresh DMEM (90 µl), the ECs were incubated with 1 mM IIIHyQ, apocynin, and PAO [34] for 2 h at 37 °C. The DMEM was removed and cells were washed two times with PBS, and fresh DMEM was then added. Finally, the cells were incubated with DHE (3 µM) for 30 min and then NADPH (100 µM) to generate $O_2^{\bullet-}$; the experiment was performed in the dark. Cell images were captured after 30 min with a Zeiss LSM 510 laser scanning confocal microscope at excitation and emission wavelengths of 520 and 610 nm, respectively.

Superoxide anion radical-scavenging capacity assay

The $O_2^{\bullet-}$-scavenging capacity of IIIHyQ was measured by competition with a molecular probe, nitroblue tetrazolium (NBT), after synthesis of $O_2^{\bullet-}$ by the hypoxanthine–xanthine oxidase (HPX–XOD) system. Briefly, 200 µl of NBT solution (0.34 mM in PBS), 500 µl of HPX (2 mM in PBS), and 100 µl of IIIHyQ prepared at the desired concentration (or the solvent-only control) were vortex-mixed for 5 s. Then, 200 µl of XOD (0.56 U/ml in PBS) was added and vortex-mixed for 30 s. Samples were taken every 10 min to measure the absorbance at 560 nm. NBT has a yellow color that upon reduction by $O_2^{\bullet-}$ forms the blue formazan.

Cell toxicity assay

Toxicity of IIIHyQ and apocynin was determined by 3-(4,5-dimethylthiazol-2-yl)-2,5-diphenyltetrazolium bromide (MTT) assay using rat adrenal medullar cells (PC-12). The cells were cultured in modified DMEM supplemented with 5% fetal bovine serum, 10% horse serum, and 1% penicillin–streptomycin. The cell suspension (110,000

cells/ml) was separated into aliquots of 90 µl in a 96-well microtiter plate (CellBIND, Corning, Lowell, MA, USA) and allowed to adhere for 24 h. Afterward, 10 µl of IIIHyQ or apocynin solution was added (to cover a range of concentrations from 0 to 1 mM, in 1% dimethyl sulfoxide (DMSO)) to the microtiter plate, and the cells were further incubated for 48 h at 37 °C. The medium was then removed, and the cells were washed with PBS. Next, DMEM (200 µl) and thiazolyl blue tetrazolium bromide (50 µl of 2.5 mg/ml) were added to each well for 3 h at 37 °C. Finally, these solutions were removed, 250 µl of DMSO was added, the plate was shaken (~75 rpm) for 20 min, and the absorbance was measured at 562 nm. The cytotoxicity values were normalized to the PBS (1% DMSO) control without IIIHyQ and apocynin.

Results and discussion

Interaction of the IIIHyQ with p47^{phox}

The mechanism of NADPH oxidase inhibition by apocynin-derived enzymatic oxidation products remains unclear. In phagocytes, myeloperoxidase is expected to convert apocynin into active metabolites [24,35,36]. Along these lines, we generated a library of potential inhibitors of NADPH oxidase, resulting in the identification of a IIIHyQ as a strong inhibitor of the human EC NADPH oxidase via blocking the interaction between p47^{phox} and p22^{phox} subunits. We hypothesized that the IIIHyQ may bind to critical Cys residues on p47^{phox} preventing its translocation to the membrane. p47^{phox} contains four Cys residues at positions 98, 111, 196, and 378. Cys196 is located within the N–SH3 domain, which binds the PRR of p22^{phox} (Fig. 1B).

To elucidate the role of specific Cys residues, and particularly Cys196 of p47^{phox} in the interaction with p22^{phox} in the presence of IIIHyQ, four mutants (C98G-p47^{phox}, C111A-p47^{phox}, C196A-p47^{phox}, and C378A-p47^{phox}) of recombinant p47^{phox} were generated. Dose–response analysis of IIIHyQ in C98G-p47^{phox} and C378A-p47^{phox} enzyme-linked immunosorbent assay (Fig. 2A) shows that the apocynin derivative disrupts the interaction with biotin-p22^{phox} giving IC_{50} values (4.9 and 2.3 µM, respectively; Fig. 2B and E) comparable to the value previously reported using the wild-type p47^{phox} (1.60 µM) [26], whereas the IC_{50} value using C111A-p47^{phox} (21.0 µM) was an order of magnitude higher (Fig. 2C). However, when Cys196 was replaced by Ala, the IIIHyQ was unable to block the interaction over the entire dose range (Fig. 2D). This was interesting, as Cys196 is the only cysteine located within the SH3 domain and particularly within the N-

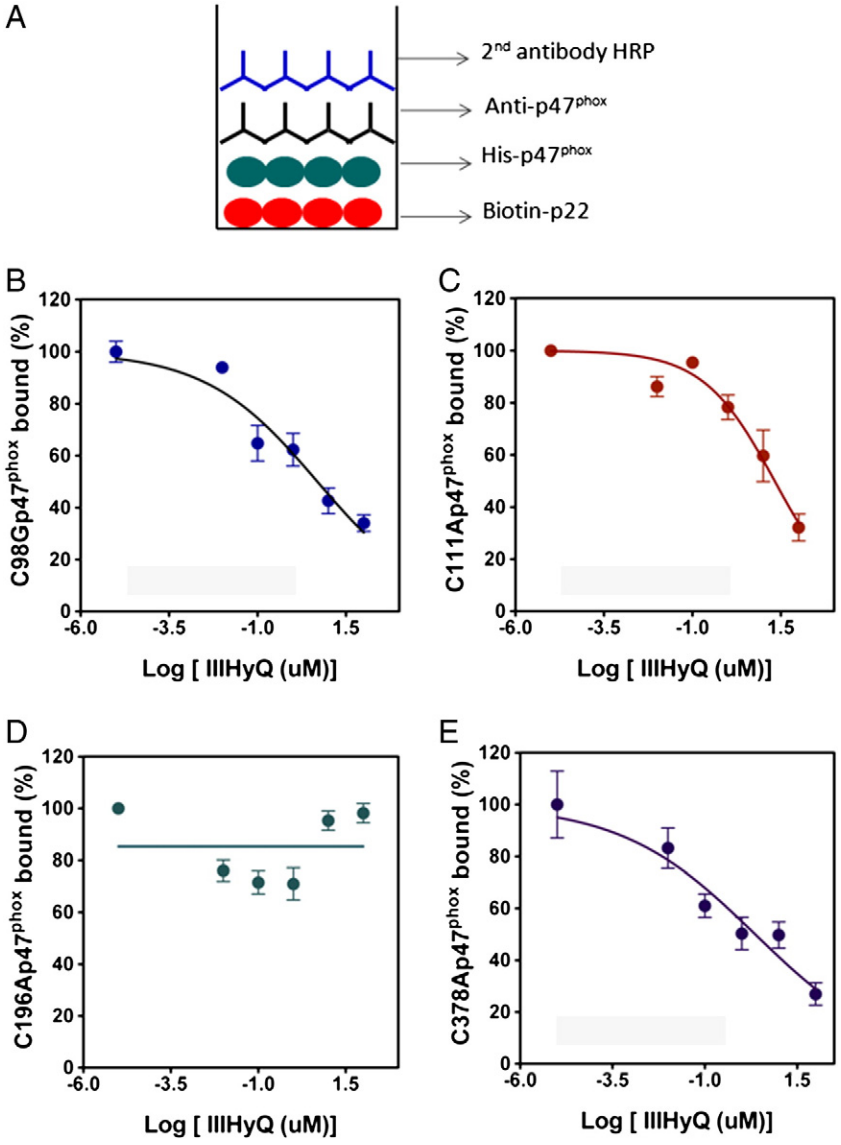

Fig. 2. Interactions between biotin-p22^{phox} and recombinant His-p47^{phox} (wild type and mutants) in the presence of IIIHyQ. (A) Scheme of the ELISA. (B) Dose response using C98G-p47^{phox} (IC_{50} 4.9 µM), (C) C111A-p47^{phox} (IC_{50} 21.0 µM), (D) C196A-p47^{phox} (IC_{50} not determined), and (E) C378A-p47^{phox} (IC_{50} 2.3 µM).

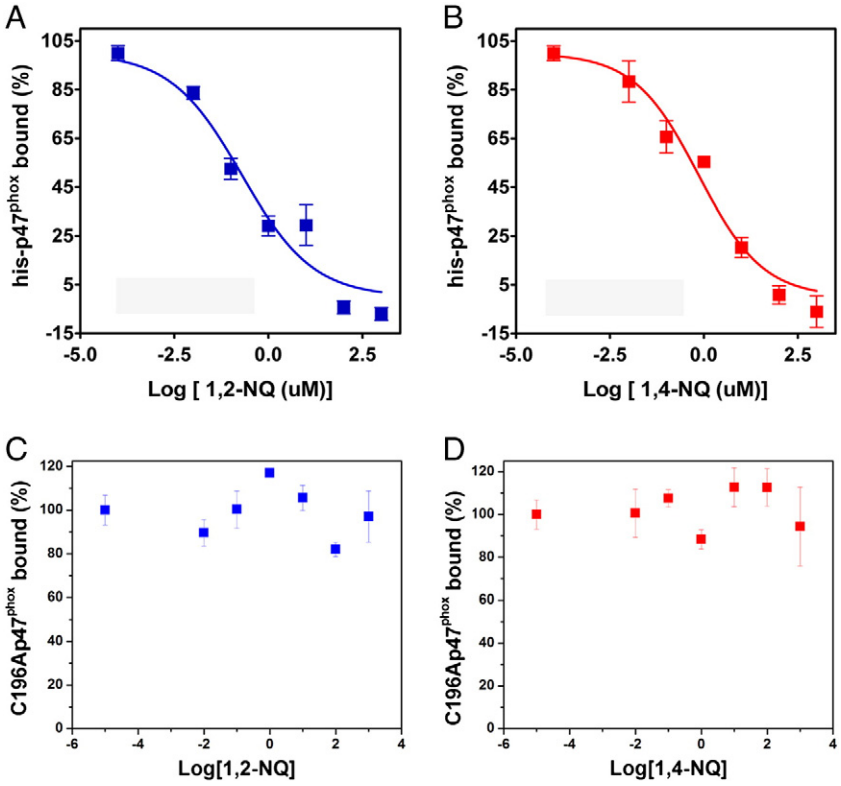

Fig. 3. ELISA controls with quinone structures. Effects of 1,2- and 1,4-naphthoquinones on the interaction between biotin-p22^{phox} and recombinant His-p47^{phox}. (A) Biotin-p22^{phox}–wild-type His-p47^{phox} interaction with 1,2-naphthoquinone (IC_{50} 0.2 μM), (B) biotin-p22^{phox}–wild-type His-p47^{phox} interaction with 1,4-naphthoquinone (IC_{50} 0.7 μM), (C) biotin-p22^{phox}–C196A-p47^{phox} interaction with 1,2-naphthoquinone, and (D) biotin-p22^{phox}–C196A-p47^{phox} interaction with 1,4-naphthoquinone (IC_{50} values of (C) and (D) were not determined).

terminal SH3 domain that binds the PRR of p22^{phox}. Cys196, therefore, seems to be a critical target for preventing protein–protein interactions necessary for NADPH oxidase activation. Several quinones (for example 1,2- and 1,4-naphthoquinones) are known to form Michael adducts with cysteine residues [28]. As controls, 1,2-naphthoquinone and 1,4-naphthoquinone were evaluated for their effects on the interaction of His-p47^{phox} with biotin-p22^{phox}. Using wild-type His-p47^{phox}, both quinones were able to prevent this protein–protein association with comparable IC_{50} values (0.2 and 0.7 μM respectively; Fig. 3A and B). However, when the mutant C196A-p47^{phox} was used, neither naphthoquinone had any effect (Fig. 3C and D).

The reactivity of the IIIHyQ on p47^{phox} Cys residues was determined using the fluorescent dye lucifer yellow iodoacetamide (Fig. 4A). The 1,2- and1,4-naphthoquinones were used as positive controls, and apocynin was used as a negative control. The fluorescence spectra (Fig. 4B) show a significant decrease (~80%) in total Cys-thiol groups after incubation with the IIIHyQ, as well as the naphthoquinones, whereas incubation with apocynin did not result in appreciable reduction in the fraction of free Cys residues. This result suggests that IIIHyQ is not selective for Cys196, which is consistent with the results of Park and Park using the fluorescent probe *N, N′*-dimethyl-*N*-(iodoacetyl)-*N′*-(7-nitrobenz-2-oxa-1,3-diazol-4-yl) ethyleneamine [37]. This and the reduction of ~80% of total cysteines indicate that the IIIHyQ is not specific for Cys196, but its modification seems to be critical to prevent the interaction with p22^{phox}.

Effect of the IIIHyQ on NADPH oxidase after enzyme activation

NADPH oxidase inhibition can be the result of at least two mechanisms. One mechanism involves interference of enzyme activation, e.g., by preventing translocation of cytosolic subunits to the cell membrane. A second mechanism involves the inhibition of the already assembled and activated enzyme. Along these lines, it is important to note that few attempts have been made to evaluate inhibition when the NADPH oxidase is already activated and the target sites for the inhibitors may be restricted. For example, PAO is ineffective as an

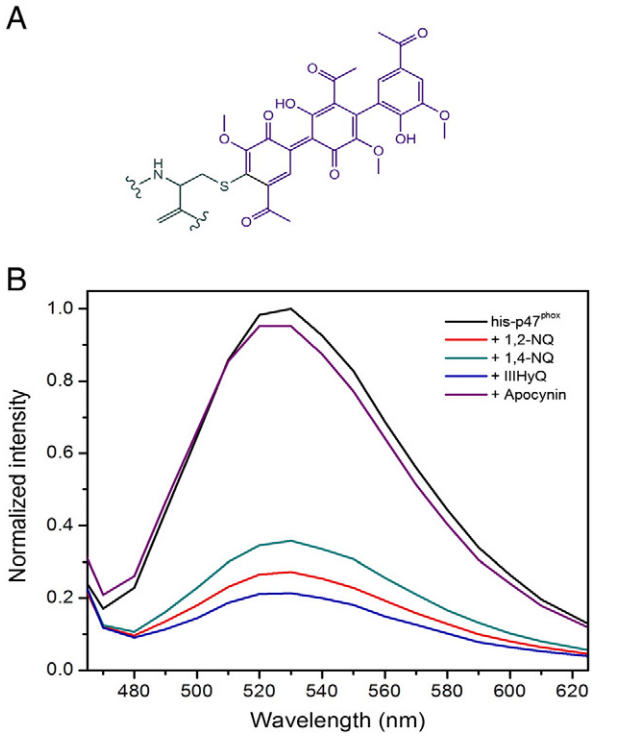

Fig. 4. Quantification of cysteines in recombinant His-p47^{phox} incubated with apocynin, IIIHyQ, 1,2-naphthoquinone, and 1,4-naphthoquinone. (A) Chemical representation of the Michael adduct between IIIHyQ and Cys thiol group. (B) Fluorescence spectra of lucifer iodoacetamide complexed with cysteines of wild-type p47^{phox}.

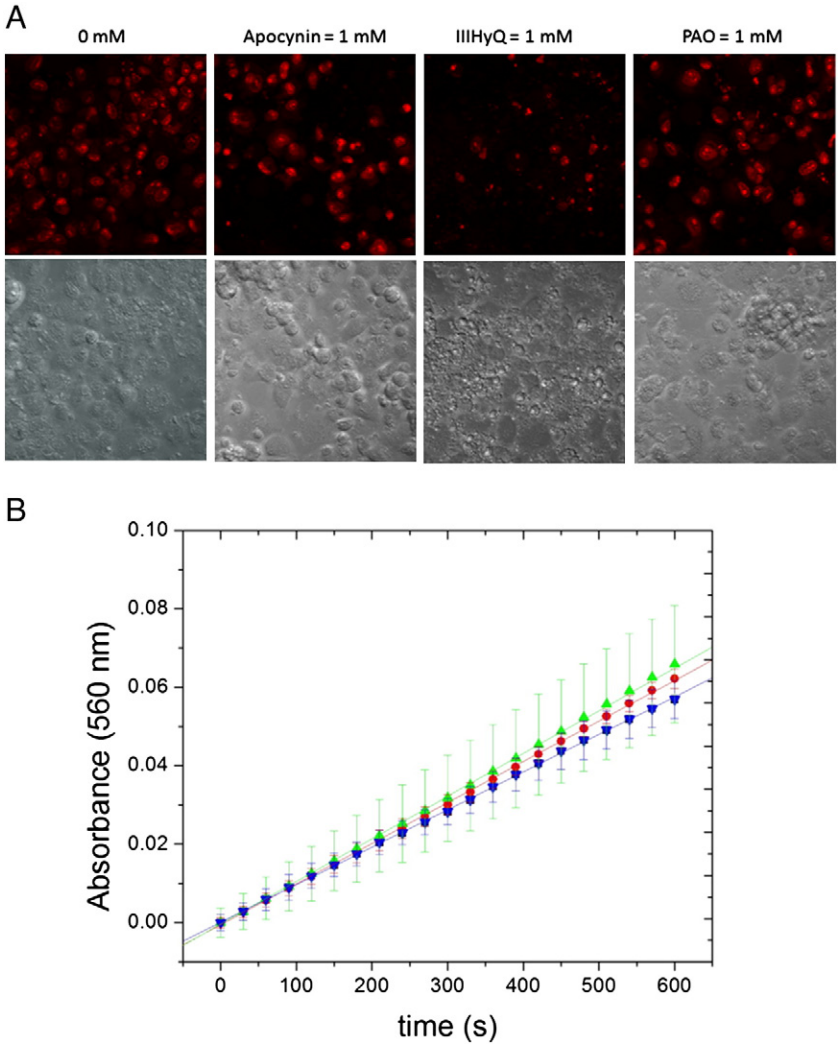

Fig. 5. (A) Intracellular $O_2^{\bullet-}$ detection by DHE staining in endothelial cells. Inhibitory activity of apocynin, IIIHyQ, and PAO on previously activated NADPH oxidase. (B) $O_2^{\bullet-}$-scavenging capacity of IIIHyQ (0–1 mM): black square, IIIHyQ 0.0 μM; red circle, IIIHyQ 0.01 μM; green triangle, IIIHyQ 100.0 μM; blue triangle, IIIHyQ 1000.0 μM.

inhibitor once NADPH oxidase is activated [38]. We proceeded to investigate whether the IIIHyQ was an effective inhibitor after NADPH oxidase activation. To that end, we activated the enzyme within ECs with PMA and followed intracellular $O_2^{\bullet-}$ formation using DHE, a cell-permeative dye that reacts with $O_2^{\bullet-}$ to generate 2-hydroxyethidium [31,33]. The production of $O_2^{\bullet-}$ was then examined upon addition of IIIHyQ. As shown in Fig. 5A, the level of $O_2^{\bullet-}$ decreased in the presence of IIIHyQ in relation to apocynin and PAO, although the inhibition was not as striking as addition of IIIHyQ before NADPH activation. Nevertheless, it is interesting that IIIHyQ can achieve some degree of inhibition once enzyme assembly had occurred. One explanation is that IIIHyQ may be able to bind to Cys196 even after the $p47^{phox}$–$p21^{phox}$ association takes place. If this occurs, then once IIIHyQ binds to Cys196, the two enzyme subunits dissociate, thereby eliminating enzyme activity. Another possibility is that other protein–inhibitor interactions take place. For example, it has been demonstrated that polyphenols have an affinity for physically interacting with the PRR of proteins and inducing conformational changes [17,18]. Interactions between the N–SH3 domain of $p47^{phox}$ and PRR of $p22^{phox}$ occur through Van der Waals and hydrogen bond interactions [9,39]. Similar interactions may occur with polyphenols that can disrupt the association of $p47^{phox}$–$p21^{phox}$. Importantly, IIIHyQ does not scavenge free radicals. Similar interactions may occur with polyphenols that can disrupt some of those interactions resulting in a reversible effect on NADPH oxidase. As a control, we determined that the IIIHyQ does not scavenge $O_2^{\bullet-}$ and the reduction of $O_2^{\bullet-}$ levels is due to a loss of enzymatic activity (Fig. 5B).

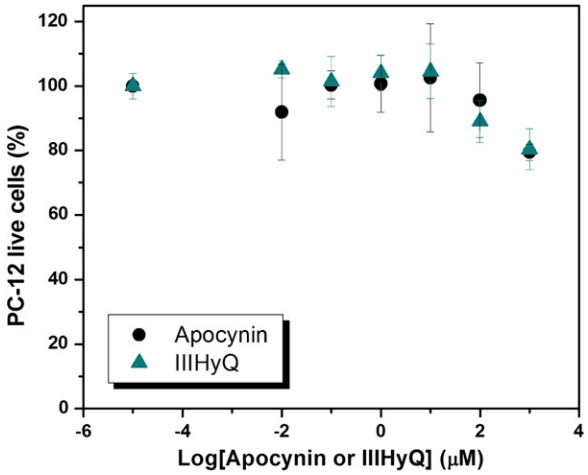

Fig. 6. MTT assay. Cytotoxicity of apocynin and IIIHyQ on rat adrenal medullar cells (PC-12).

Toxicity of apocynin and IIIHyQ

Our results suggest that IIIHyQ does not target a specific cysteine and thus may be indiscriminately reactive toward other cysteines residues on other proteins within cells, thereby affecting critical pathways that may damage or kill cells. We therefore evaluated the cytotoxicity of IIIHyQ via the standard MTT assay using PC-12 cells. As shown in Fig. 6, the dose–response plots of apocynin and IIIHyQ were similar and only a 20% loss in viability occurred at a concentration of 1 mM. This value is far higher than the IC_{50} values obtained during the NADPH oxidase activity assay (30 nM) and for biotin-$p22^{phox}$–$p47^{phox}$ (1.60 μM) [26], indicating a potentially wide therapeutic window. These cytotoxicity results are similar to those for the stilbene resveratrol and its peroxidase-generated oxidation products [40].

Conclusions

We have studied the mechanism of inhibition of the IIIHyQ derived enzymatically from apocynin, with specific attention given to the interaction of $p22^{phox}$ and $p47^{phox}$. Cysteine residues of $p47^{phox}$ seem to be the primary target for the quinone, with Cys196 in the N–SH3 domain playing a critical role as a site of inhibition. Specifically, the IIIHyQ is ineffective when Cys196 is replaced by alanine. The IIIHyQ also reacts with other Cys residues in $p47^{phox}$; however, inhibition is eliminated only when a likely Michael addition to Cys196 occurs. Similar results were obtained with the structurally simpler 1,2- and 1,4-naphthoquinones. Despite the relatively low selectivity of the IIIHyQ on Cys residues, the compound showed minimal cytotoxicity in vitro. Enzymatic oligomerization of apocynin represents an attractive alternative to generate potential inhibitors of NADPH oxidase. Characterization of IIIHyQ and its mechanism of action provides additional insight into the structural features for potent inhibitors of vascular NADPH oxidase, which may prove valuable in the search for effective therapeutic interventions in cardiovascular diseases related to oxidative stress [34].

Acknowledgments

This work was supported by the National Institutes of Health (AT002115). We are grateful to Dr. Christopher Bjornsson, Director of the Microscopy and Imaging Core Facility (Center for Biotechnology and Interdisciplinary Studies, Rensselaer Polytechnic Institute), for his help with confocal fluorescence microscopy analysis.

References

[1] Babior, B. M. NADPH oxidase: an update. *Blood* **93:**1464–1476; 1999.
[2] Guzik, T. J.; Harrison, D. G. Vascular NADPH oxidases as drug targets for novel antioxidant strategies. *Drug Discov. Today* **11:**524–533; 2006.
[3] Li, J. M.; Mullen, A. M.; Shah, A. M. Phenotypic properties and characteristics of superoxide production by mouse coronary microvascular endothelial cells. *J. Mol. Cell. Cardiol.* **33:**1119–1131; 2001.
[4] Brandes, R. P.; Kreuzer, J. R. Vascular NADPH oxidases: molecular mechanisms of activation. *Cardiovasc. Res.* **65:**16–27; 2005.
[5] Kuroda, J.; Nakagawa, K.; Yamasaki, T.; Nakamura, K.; Takeya, R.; Kuribayashi, F.; Imajoh-Ohmi, S.; Igarashi, K.; Shibata, Y.; Sueishi, K.; Sumimoto, H. The superoxide-producing NAD(P)H oxidase Nox4 in the nucleus of human vascular endothelial cells. *Genes Cells* **10:**1139–1151; 2005.
[6] Martyn, K. D.; Frederick, L. M.; von Loehneysen, K.; Dinauer, M. C.; Knaus, U. G. Functional analysis of Nox4 reveals unique characteristics compared to other NADPH oxidases. *Cell. Signal.* **18:**69–82; 2006.
[7] Li, J. M.; Fan, L. M.; George, V. T.; Brooks, G. Nox2 regulates endothelial cell cycle arrest and apoptosis via p21 (cip1) and p53. *Free Radic. Biol. Med.* **43:**976–986; 2007.
[8] Ago, T.; Kuribayashi, F.; Hiroaki, H.; Takeya, R.; Ito, T.; Kohda, D.; Sumimoto, H. Phosphorylation of p47(phox) directs phox homology domain from SH3 domain toward phosphoinositides, leading to phagocyte NADPH oxidase activation. *Proc. Natl. Acad. Sci. U. S. A.* **100:**4474–4479; 2003.
[9] Groemping, Y.; Lapouge, K.; Smerdon, S. J.; Rittinger, K. Molecular basis of phosphorylation-induced activation of the NADPH oxidase. *Cell* **113:**343–355; 2003.
[10] Li, J. M.; Shah, A. M. Differential NADPH- versus NADH-dependent superoxide production by phagocyte-type endothelial cell NADPH oxidase. *Cardiovasc. Res.* **52:**477–486; 2001.
[11] Gorlach, A.; Brandes, R. P.; Nguyen, K.; Amidi, M.; Dehghani, F.; Busse, R. A gp91phox containing NADPH oxidase selectively expressed in endothelial cells is a major source of oxygen radical generation in the arterial wall. *Circ. Res.* **87:**26–32; 2000.
[12] Sumimoto, H.; Kage, Y.; Nunoi, H.; Sasaki, H.; Nose, T.; Fukumaki, Y.; Ohno, M.; Minakami, S.; Takeshige, K. Role of Src homology-3 domains in assembly and activation of the phagocyte NADPH oxidase. *Proc. Natl. Acad. Sci. U. S. A.* **91:**5345–5349; 1994.
[13] Touyz, R. M.; Briones, A. M. Reactive oxygen species and vascular biology: implications in human hypertension. *Hypertens. Res.* **34:**5–14; 2011.
[14] Selemidis, S.; Dusting, G. J.; Peshavariya, H.; Kemp-Harper, B. K.; Drummond, G. R. Nitric oxide suppresses NADPH oxidase-dependent superoxide production by S-nitrosylation in human endothelial cells. *Cardiovasc. Res.* **75:**349–358; 2007.
[15] Cayatte, A. J.; Rupin, A.; Oliver-Krasinski, J.; Maitland, K.; Sansilvestri-Morel, P.; Boussard, M. F.; Wierzbicki, M.; Verbeuren, T. J.; Cohen, R. A. S17834, a new inhibitor of cell adhesion and atherosclerosis that targets NADPH oxidase. *Arterioscler. Thromb. Vasc. Biol.* **21:**1577–1584; 2001.
[16] Shi, J. S.; Ross, C. R.; Leto, T. L.; Blecha, F. PR-39, a proline-rich antibacterial peptide that inhibits phagocyte NADPH oxidase activity by binding to Src homology 3 domains of p47(phox). *Proc. Natl. Acad. Sci. U. S. A.* **93:**6014–6018; 1996.
[17] Asquith, T. N.; Uhlig, J.; Mehansho, H.; Putman, L.; Carlson, D. M.; Butler, L. Binding of condensed tannins to salivary proline-rich glycoproteins: the role of carbohydrate. *J. Agric. Food Chem.* **35:**331–334; 1987.
[18] Mehansho, H.; Butler, L. G.; Carlson, D. M. Dietary tannins and salivary proline-rich proteins—interactions, induction, and defense-mechanisms. *Annu. Rev. Nutr.* **7:**423–440; 1987.
[19] Heumuller, S.; Wind, S.; Barbosa-Sicard, E.; Schmidt, H.; Busse, R.; Schroder, K.; Brandes, R. P. Apocynin is not an inhibitor of vascular NADPH oxidases but an antioxidant. *Hypertension* **51:**211–217; 2008.
[20] Johnson, D. K.; Schillinger, K. J.; Kwait, D. M.; Hughes, C. V.; McNamara, E. J.; Ishmael, F.; O'Donnell, R. W.; Chang, M. M.; Hogg, M. G.; Dordick, J. S.; Santhanam, L.; Ziegler, L. M.; Holland, J. A. Inhibition of NADPH oxidase activation in endothelial cells by ortho-methoxy-substituted catechols. *Endothelium* **9:**191–203; 2002.
[21] Castor, L. R. G.; Locatelli, K. A.; Ximenes, V. F. Pro-oxidant activity of apocynin radical. *Free Radic. Biol. Med.* **48:**1636–1643; 2010.
[22] Simons, J. M.; Thart, B. A.; Ching, T.; Vandijk, H.; Labadie, R. P. Metabolic-activation of natural phenols into selective oxidative burst agonists by activated human neutrophils. *Free Radic. Biol. Med.* **8:**251–258; 1990.
[23] Thallas-Bonke, V.; Thorpe, S. R.; Coughlan, M. T.; Fukami, K.; Yap, F. Y. T.; Sourris, K. C.; Penfold, S. A.; Bach, L. A.; Cooper, M. E.; Forbes, J. M. Inhibition of NADPH oxidase prevents advanced glycation end product-mediated damage in diabetic nephropathy through a protein kinase C-alpha-dependent pathway. *Diabetes* **57:**460–469; 2008.
[24] Kanegae, M. P. P.; Condino-Neto, A.; Pedroza, L. A.; de Almeida, A. C.; Rehder, J.; da Fonseca, L. M.; Ximenes, V. F. Diapocynin versus apocynin as pretranscriptional inhibitors of NADPH oxidase and cytokine production by peripheral blood mononuclear cells. *Biochem. Biophys. Res. Commun.* **393:**551–554; 2010.
[25] Kanegae, M. P. P.; da Fonseca, L. M.; Brunetti, I. L.; Silva, S. O.; Ximenes, V. F. The reactivity of ortho-methoxy-substituted catechol radicals with sulfhydryl groups: contribution for the comprehension of the mechanism of inhibition of NADPH oxidase by apocynin. *Biochem. Pharmacol.* **74:**457–464; 2007.
[26] Mora-Pale, M.; Weiwer, M.; Yu, J.; Linhardt, R. J.; Dordick, J. S. Inhibition of human vascular NADPH oxidase by apocynin derived oligophenols. *Bioorg. Med. Chem.* **17:**5146–5152; 2009.
[27] Valente, C.; Moreira, R.; Guedes, R. C.; Iley, J.; Jaffar, M.; Douglas, K. T. The 1,4-naphthoquinone scaffold in the design of cysteine protease inhibitors. *Bioorg. Med. Chem.* **15:**5340–5350; 2007.
[28] Briggs, M. K.; Desavis, E.; Mazzer, P. A.; Sunoj, R. B.; Hatcher, S. A.; Hadad, C. M.; Hatcher, P. G. A new approach to evaluating the extent of Michael adduct formation to PAH quinones: tetramethylammonium hydroxide (TMAH) thermochemolysis with GC/MS. *Chem. Res. Toxicol.* **16:**1484–1492; 2003.
[29] Antoniotti, S.; Santhanam, L.; Ahuja, D.; Hogg, M. G.; Dordick, J. S. Structural diversity of peroxidase-catalyzed oxidation products of o-methoxyphenols. *Org. Lett.* **6:**1975–1978; 2004.
[30] Dahan, I.; Issaeva, I.; Gorzalczany, Y.; Sigal, N.; Hirshberg, M.; Pick, E. Mapping of functional domains in the p22(phox) subunit of flavocytochrome b(559) participating in the assembly of the NADPH oxidase complex by "peptide walking". *J. Biol. Chem.* **277:**8421–8432; 2002.
[31] Wind, S.; Beuerlein, K.; Armitage, M. E.; Taye, A.; Kumar, A. H. S.; Janowitz, D.; Neff, C.; Shah, A. M.; Wingler, K.; Schmidt, H. H. H. W. Oxidative stress and endothelial dysfunction in aortas of aged spontaneously hypertensive rats by NOX1/2 is reversed by NADPH oxidase inhibition. *Hypertension* **56:**490–497; 2010.
[32] Zhao, H.; Kalivendi, S.; Zhang, H.; Joseph, J.; Nithipatikom, K.; Vásquez-Vivar, J.; Kalyanaraman, B. Superoxide reacts with hydroethidine but forms a fluorescent product that is distinctly different from ethidium: potential implications in intracellular fluorescence detection of superoxide. *Free Radic. Biol. Med.* **34:**1359–1368; 2003.
[33] Zielonka, J.; Vasquez-Vivar, J.; Kalyanaraman, B. Detection of 2-hydroxyethidium in cellular systems: a unique marker product of superoxide and hydroethidine. *Nat. Protoc.* **3:**8–21; 2008.
[34] Doussiere, J.; Poinas, A.; Blais, C.; Vignais, P. V. Phenylarsine oxide as an inhibitor of the activation of the neutrophil NADPH oxidase—identification of the beta subunit of the

flavocytochrome b component of the NADPH oxidase as a target site for phenylarsine oxide by photoaffinity labeling and photoinactivation. *Eur. J. Biochem.* **251:**649–658; 1998.

[35] Lu, X. Y.; Wan, S. N.; Jiang, J.; Jiang, X. J.; Yang, W. J.; Yu, P.; Xu, L. P.; Zhang, Z. J.; Zhang, G. X.; Shan, L. C.; Wang, Y. Q. Synthesis and biological evaluations of novel apocynin analogues. *Eur. J. Med. Chem.* **46:**2691–2698; 2011.

[36] Ximenes, V. F.; Kanegae, M. P. P.; Rissato, S. R.; Galhiane, M. S. The oxidation of apocynin catalyzed by myeloperoxidase: proposal for NADPH oxidase inhibition. *Arch. Biochem. Biophys.* **457:**134–141; 2007.

[37] Park, H. S.; Park, J. W. Fluorescent labeling of the leukocyte NADPH oxidase subunit p47phox: evidence for amphiphile-induced conformational changes. *Arch. Biochem. Biophys.* **360:**165–172; 1998.

[38] Cabec, V. R. L.; Maridonneau-Parini, I. Complete and reversible inhibition of NADPH oxidase in human neutrophils by phenylarsine oxide at a step distal to membrane translocation of the enzyme subunits. *J. Biol. Chem.* **270:**2067–2073; 1995.

[39] Ogura, K.; Nobuhisa, I.; Yuzawa, S.; Takeya, R.; Torikai, S.; Saikawa, K.; Sumimoto, H.; Inagaki, F. NMR solution structure of the tandem Src homology 3 domains of p47(phox) complexed with a p22(phox)-derived proline-rich peptide. *J. Biol. Chem.* **281:**3660–3668; 2006.

[40] Ladiwala, A. R. A.; Mora-Pale, M.; Lin, J. C.; Bale, S. S.; Fishman, Z. S.; Dordick, J. S.; Tessier, P. M. Polyphenolic glycosides and aglycones utilize opposing pathways to selectively remodel and inactivate toxic oligomers of amyloid β. *ChemBioChem* **12:**1749–1758; 2011.